frontiers | Frontiers in Marine Science

TYPE Original Research
PUBLISHED 18 August 2022
DOI 10.3389/fmars.2022.909457

OPEN ACCESS

EDITED BY
Dongyan Liu,
East China Normal University, China

REVIEWED BY
Jun Gong,
Sun Yat-sen University, China
Wuchang Zhang,
Institute of Oceanology (CAS), China

*CORRESPONDENCE
Emilia Trudnowska
emilia@iopan.pl

SPECIALTY SECTION
This article was submitted to Marine Ecosystem Ecology, a section of the journal Frontiers in Marine Science

RECEIVED 31 March 2022
ACCEPTED 25 July 2022
PUBLISHED 18 August 2022

CITATION
Trudnowska E, Dragańska-Deja K, Sagan S and Błachowiak-Samołyk K (2022) Cells of matter and life – towards understanding the structuring of particles and plankton patchiness in the Arctic fjords.
Front. Mar. Sci. 9:909457.
doi: 10.3389/fmars.2022.909457

Cells of matter and life – towards understanding the structuring of particles and plankton patchiness in the Arctic fjords

Emilia Trudnowska[1]*, Katarzyna Dragańska-Deja[2], Sławomir Sagan[2] and Katarzyna Błachowiak-Samołyk[1]

[1]Marine Ecology Department, Institute of Oceanology Polish Academy of Sciences, Sopot, Poland, [2]Department of Marine Physics, Institute of Oceanology Polish Academy of Sciences, Sopot, Poland

As the environmental conditions are typically not homogenous, especially in coastal regions, they must provide a mosaic of distinct habitats that can be occupied by particles and plankton in a characteristic way. Here we analyze and map the spatio-temporal distribution patterns and the internal structure of 94 patches of various size fractions of particles and plankton studied by fine resolution measurements of two compatible laser counters performed in the upper epipelagial of two Arctic fjords over six summer seasons. Detected patches generally occupied only the minor part of the studied upper water column (on average 12%), and frequently occurred as multi-size-fraction forms. The observed concentrations within the patches were mostly 1.6 times higher than the background concentrations (max 4.1). The patches ranged in size horizontally from 1 to 92 km (median length 12 km) and vertically from 5 to 50 m (median 26 m). Because the designated patches varied in terms of their shapes and internal structure, a novel classification approach to of patches is proposed. Accordingly, seven types of patches were distinguished: Belt, Triangle, Diamond, Flare, Fingers, Flag, and Rosette. The particles and plankton exhibited all types of these distribution patterns, regardless of the size fraction and location. The observed steepening size spectra slopes over years implies that proliferating Atlantic water advection, triggering increasing role of the smallest size fractions, played the crucial role on compositional dynamics on temporal scale. The recurring high concentration patches of particles and plankton near glaciers suggest that their melting, together with biological production, were the strongest factors generating patchiness on the local scale. An observed under several occasions depth differentiation among size fractions building together vertically thin multi-size-fraction patches is an interesting feature for further studies. Even if distribution patterns of particles and plankton did not clearly reflect all patterns in the environmental water structuring, they happened to be related to the presence of glacier runoff, eddy, sea mountain and hot spots of chlorophyll fluorescence.

KEYWORDS

particles, plankton, distribution, patchiness, size, Arctic, fjords

Introduction

Distribution of particles and plankton in the oceans is highly patchy. Those 'clouds of matter' are fundamental 'cells' for trophic interactions and organic carbon cycling (Brentnall et al., 2003; Benoit-Bird et al., 2011; Godø et al., 2012; Priyadarshi et al., 2019), as their distribution arranges many elements of marine ecosystems, e.g., the hotspots of fisheries, or the massive vectors of carbon pump. The identification of the phenomenon of patchiness is not new to ecological plankton studies (Wiebe et al., 1968; Levin and Segel, 1976; Mackas et al., 1985), with numerous examples that succeeded in exposing the existence of spatial heterogeneity in plankton distribution patterns (Davis et al., 1991; Franks, 2005; Genin et al., 2005; Prairie et al., 2010; Lévy et al., 2018; Briseño-Avena et al., 2020). Although patches of particles and plankton are commonly observed in marine systems, we still know little about their composition and internal structure (Kotliar and Wiens, 1990; Currie et al., 1998).

The possibility to observe and thus document the patchiness has opened just recently, thanks to the high resolution automatic instruments such as underwater cameras, laser counters and acoustic methods (Davis et al., 2005; Möller et al., 2012; Trudnowska et al., 2012; Trudnowska et al., 2016; Geoffroy et al., 2017; Robinson et al., 2021). However, in most cases the patches of only one type or fraction of particles or plankton could be studied, mostly due to the methodological constraints, as every single method is limited to specific type/size of objects. The simultaneous application of the combination of various instruments, dedicated to different size fractions of particles and plankton, opened up the possibility of traceability of the full composition of those 'cells of matter and life' (Stemmann et al., 2008; Forest et al., 2012; Trudnowska et al., 2018; Lombard et al., 2019; Szeligowska et al., 2020). Moreover, such an approach gives a unique possibility to check, if those patches are multi-size-fractioned or rather monospecific in terms of dominating size fraction.

A co-distribution of plankton and particles in marine realm is a derivative of many physical and biological processes that all occur at different spatio-temporal scales (Pinel-Alloul, 1995; Prairie et al., 2012; Mahadevan, 2016; Trudnowska et al., 2020a). The attempts to study patchiness patterns of particles and plankton distribution together with underlying physical and biophysical fields suggested that the observed heterogeneity at both spatial and temporal scales is an effect of the jointed forcing of such physical mechanisms as e.g., ocean turbulence, mixing, currents combined with ecological interactions such as e.g., predator-prey encounter rates (Lovejoy et al., 2001; Seuront et al., 2001; Schmitt and Seuront, 2008). It was also related to specific physical features enhancing particles and plankton aggregations, such as ocean fronts and eddies (Durham and Stocker, 2012; Greer et al., 2016; Trudnowska et al., 2016), vertical thermal stratification (McManus et al., 2005; Steinbuck et al., 2009; Greer et al., 2013), river input (Matsuoka et al., 2012; Ehn et al., 2019), or the contact with sea ice (Trudnowska et al., 2018). Owing to those numerous studies providing a long list of mechanisms favoring generation of patches, it is now recognized that there is a continuing need to study and characterize the small-scale biological-physical interactions between particles/plankton and their local environment, as well as the scaled-up effects of these small-scale interactions on larger-scale dynamics (Nayak et al., 2021).

As the environmental conditions are typically not homogenous, especially in coastal regions, they must provide a mosaic of distinct habitats that can be occupied by a characteristic set of particle types and plankton species. One of the interesting and valuable systems to study this phenomenon are Arctic fjords, where the dynamics of the hydrographic situation is shaped by the advected warm, saline and biologically rich Atlantic waters that collide with the outflow of cold, fresh and turbid waters from the melting glaciers (Svendsen et al., 2002; Nilsen et al., 2008; Cottier et al., 2010; Pavlov et al., 2013; Skogseth et al., 2020), that enrich water with nutrients (Halbach et al., 2019; McGovern et al., 2020). Such strong hydrographical gradients set an interesting scene for studies how plankton and particles (both living and non-living) are portioning the water horizontally and vertically. This high spatial variability in distribution patterns of particles and plankton result in pronounced spatial gradients in primary and secondary production (Piwosz et al., 2009; Trudnowska et al., 2014). Both Kongsfjorden (KONG) and Isfjorden (ISF) undergo seasonal shifts between dominating Arctic and Atlantic states, represented not only by the balance in physical water properties (Svendsen et al., 2002) but also by the presence of fauna and flora associated with those two regimes (Hop et al., 2006). Due to the co-existence of Atlantic, Arctic, and freshwater sources in fjords the observed interactions between endemic Arctic species with boreal ones have wide ecological and biogeochemical implications (Hop et al., 2002; McGovern et al., 2020). Hence, the fjords along the west coast of Spitsbergen are sensitive indicators of environmental fluctuations and are often treated as model sites to study the

effects of climate changes on marine ecosystems. Indeed, the progressing "Atlantification" of the west Spitsbergen fjords is highly modifying the timing of phytoplankton bloom periods (Hodal et al., 2012; Hegseth and Tverberg, 2013), community compositions of protists (Kubiszyn et al., 2014; Smoła et al., 2017) and zooplankton (Gluchowska et al., 2016; Trudnowska et al., 2020b), influencing finally the overall food web interactions in the fjords (Węsławski et al., 2017; Vihtakari et al., 2018; Csapó et al., 2021), leading in consequence to substantial burial of organic carbon (Avila et al., 2012; Smith et al., 2015; Zaborska et al., 2018). Moreover, those glacier-impacted fjord parts constitute important nurseries and feeding areas for fish, seabirds and marine mammals (Lydersen et al., 2014; Urbanski et al., 2017).

This study addresses a recognized requirement for new insight studies at the interactions between ocean physics and ecology in structuring marine ecosystems (Lévy et al., 2018; Borja et al., 2020; Nayak et al., 2021). It was addressed by monitoring the patterns of patchiness of a wide spectrum of particles and plankton within the upper epipelagial by the observations made *via* high resolution technology (laser counters) over several summer seasons in two Arctic fjords. Because the formation, existence and distribution of patches determine both the biomass distribution and energy transfer through marine food webs as well as relate to the environmental disturbances (e.g., eddies, high turbidity), the efforts of scaling up our perception of micro-scale distribution of particles and plankton distribution over large-scale transects oscillated around the question, whether patterns of their patchiness are recurring. Therefore, a goal of this study was to find elucidations and answers for a few questions: 1) Does the distribution of particles and plankton patches differ over time and space? 2) What is the spatial scale of particles and plankton patchiness? 3) Are patches of various size fractions of particles and plankton co-occurring? 4) Does the internal structure of particles and plankton patches differ?

Methods

Study area

To study thoroughly a patchiness of particles and plankton, we used 11 transects investigated in two fjords of the western Spitsbergen, Kongsfjorden (KONG) and Isfjorden (ISF) (Figure 1), where numerous long-term monitoring programs are performed. Surveys were performed yearly during summer (late July – early August Supplementary Table 1). In KONG, transects either started from the very outer parts from the West Spitsbergen

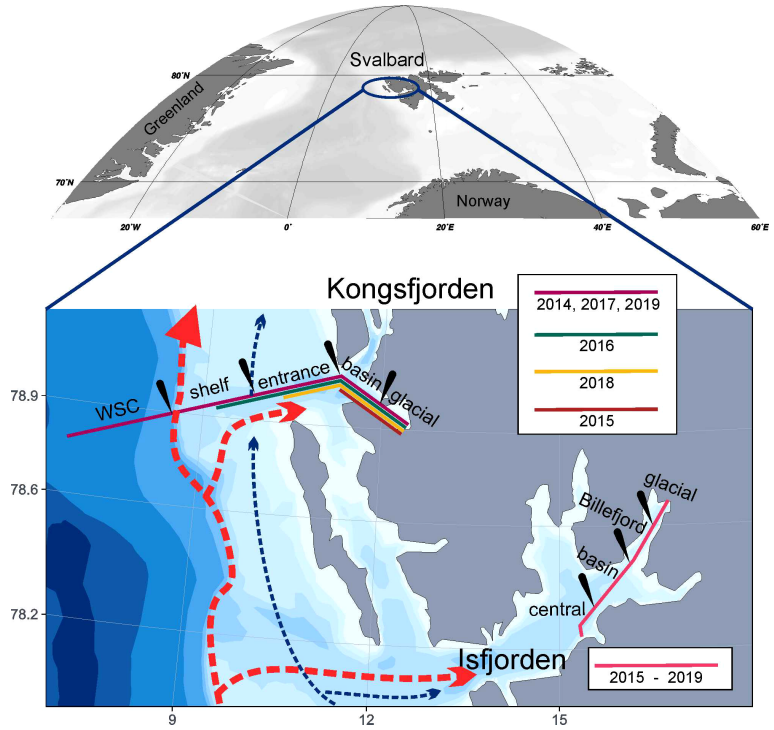

FIGURE 1
Map of the studied area: Kongsfjorden and Isfjorden (Svalbard). The ranges of transects in particular years are marked with colors. Black ticks indicate sub-regions for grouping presented at Figure 3.

Current domain (2014, 2017, 2019) or from more coastal parts of the shelf (2015, 2016, 2018) (Figure 1), and spanned towards the innermost glacial bay. The sampling in ISF was much more consistent over years as exactly the same lengths of the transects over 2015 – 2019 summer seasons were investigated. However, they were restricted to the fjord's interior. Data from KONG has not been published before, whereas the background measurements from the ISF transect were recently published (Szeligowska et al., 2020). Both fjords are characterized by the advection of Atlantic origin water in the outer parts and by the freshwater runoff of several glaciers and glacier-fed rivers in the inner parts. They both are treated as natural laboratories for international, long-term monitoring of Spitsbergen marine environment (Wiencke and Hop, 2016), and thus serve as valuable reference sites on the way to the Arctic Ocean.

Sampling

The high-resolution measurements (Supplementary Figure 1) of wide size range of particles and plankton distribution were performed in an undulating mode between surface and 50 m depth. The sampling platform was towed from the research vessel Oceania at speed ranging from 2.5 up to 4 kn (1.3 – 2 m/s), depending on weather and ice conditions. In consequence, the cycle of descent/ascent with ~0.33 m/s down to 50 m resulted in distance of a diving cycle ranging between 400 m and 800 m. In Isfjorden a towing distance was sometimes larger (up to 1 500 m), because of a deeper oscillatory towing (to 80 m)". The sampling platform was equipped with two laser-based optical counters: Laser *In Situ* Scattering and Transmissometry instrument (LISST-100X, type B, Sequoia Scientific, Inc., WA, United States) and a Laser Optical Plankton Counter (LOPC, Brooke Ocean Technology Dartmouth, Canada) and supplemented by a conductivity-temperature-depth (CTD, SBE 911plus, Seabird Electronics Inc., United States) and a fluorometer (Seapoint Sensors Inc., United States) sensors. Because both the LISST and the LOPC cannot distinguish between living plankton, detritus, and other non-living suspensions, the assessed concentrations of a wide size range of particles and plankton (between 1 µm to 10 mm) are presented as size-resolved fractions: Pico (1-3 µm), Nano (3–20 µm), Micro (20–200 µm), Small (200 – 500 µm), Medium (500 – 1 000 µm) and Large (1 000 – 10 000 µm). The lower detection limit of LISST instrument *(<3 µm)* should be treated with caution and here it represents the 'Pico' fraction. In consequence a slightly narrower size range of the Nano fraction (3-20 µm instead of 2-20 µm) was set, which is in accordance to our previous studies (Trudnowska et al., 2018; Szeligowska et al., 2020).

Calculations and visualizations

To ensure the high quality of data we performed procedures for QAQC. Quality Assurance (QA) was obtained by cleaning the lens of instruments to avoid a light distraction on dust/contaminants. The accuracy of the measurements was tested before the cruise in the lab. Moreover, the background was set for LISST by performing measurements with miliQ water just before deployments. Quality Control (QC) was adopted by screening raw data to eliminate errors, anomalous values and all kind of outliers. In LISST data background corrections were applied. Once raw measurements were cleaned, data were structured (averaged) over 1-m depth intervals (Supplementary Figure 1) and over 0.05 longitude for patches assignment and over 0.2 longitude for size spectra calculations.

Size spectra were calculated as the concentrations of particles and plankton within logarithmically increasing size intervals (32 size classes of LISST data, 49 size classes of LOPC data), normalized to the widths of those size classes. In the double logarithmic coordinates (log-log space: log(concentration), log (size)), a straight line was fitted to the spectra by the least square fitting method. The intercept (exponent a of the fitting) and slope (exponent b of the fitting) of such a normalized size spectrum are indicators for abundance and structure of particles and plankton communities, respectively. A high intercept of a spectrum is caused by high abundances. Steep slope of a spectrum indicates communities with domination of smaller size fractions, while flatter slopes of the spectra indicate the high relative importance of larger size fractions. Ecologically, flatter spectra are observed in systems where there is more recycling of biomass (Zhou, 2006), while steeper ones are observed in ecosystems with a relatively high loss of energy from primary producers to secondary consumers (Boudreau et al., 1991), in form of longer food chains, but also with an efficient energy transfer between trophic levels (Zhou et al., 2010; Barnes et al., 2010; Blanchard et al., 2017). Differences in size spectra slopes over sub-regions and studied years were tested by the two-way ANOVA.

The mean abundance and standard deviation (sd) was calculated for each size fraction in each transect (separately fjords and years) in order to designate a concentration threshold of patches. Consequently, the patch threshold is fjord- and year-specific. Data points were assigned as 'patches' in accordance to the rule applied in the previous studies (Piontkovski et al., 1997; Trudnowska et al., 2016), i.e., as the ones that had higher concentrations than a threshold (mean abundance + sd). The location of individual patches was presented by the 2D kernel density estimation ('stat_density_2d' function in R) applied to x-y coordinates (longitude and depth) of the data points assigned as 'patches'. In order to distinguish the individual patches from each other, the hierarchical clustering ('res.hc' function of "factoextra" package in R) of their x-y coordinates (longitude and depth) was performed to group together data points that lay close by and to eliminate the outlier observations (because sometimes only the singular high concentration data points were scattered in the gridded space of data points). The percentage of the data points representing patches of particular size fractions in particular fjords and summer

seasons was calculated as the ratio between the data points designated as patches (N in Supplementary Table 2) to the total number of data points in particular transect. Each analyzed patch was ascribed to specific type depending on its shape and the location of its core (the location of the hot spot of kernel density). In consequence after a long process of looking thoughtfully at each detected shape, a 'taxonomy of patches' was proposed, by distinguishing 7 various types of patches:

- Belt - narrow and elongated shape, kernel density located in the central part
- Triangle - wider shape at one side of the location of density hot spot and narrowing towards the other side, kernel density located at the wider side
- Diamond - wider shape at the middle and narrowing towards the ends, kernel density located in the central part
- Flare - narrow shape at side with the density hot spot and widening towards the other side of lower concentration, kernel density located at the border of narrow part
- Fingers - Flare type split into two or more parts
- Flag - narrow and elongated shape with some extension near surface, no clear kernel density location
- Rosette - rounded shape, kernel density located in the central part and the lowering concentrations symmetrically spaced

We regard a proposition of such classification of patches as an additional derivative of this study that is a potentially interesting aspect to be developed in further research. Because the applied laser optical counters cannot discriminate between living and non-living objects, it should be emphasized that the designated patches are composed of both particles of various origin and plankton belonging to different species/genus. Indices of the spatial heterogeneity (Lloyd's crowding index, Lloyd's patchiness index) were calculated according to the previously published formulas (Pinel-Alloul, 1995), in which the variance (s^2) is related to the mean (m) of particles and plankton concentrations in patches (Lloyd's crowding index: $m+(s^2/m)-1$; Lloyd's patchiness index: $1+s^2-m^{-1}$). Such an approach is based on the assumptions of the Poisson random distribution model, which corresponds to spatial homogeneity and variance to mean ratios.

Because quite different environmental conditions and spatial coverage of sampling concerned both studied areas, we decided to analyze the statistical trends separately for individual fjords. We analyzed the cross correlations (Pearson) between patch characteristics (depth range, horizontal length, area, size spectrum), environmental settings (temperature, salinity, chlorophyll), spatial heterogeneity indices (logarithms of variance/mean ratio, Lloyd's crowding and patchiness indices), and concentrations of particular size fractions of particles and plankton (log10()). The strength of the correlation is marked on the corrplot as the size of the dot and the direction of the correlation is marked with a color (positive is blue, negative is red).

DistLM (distance-based linear model) routines were run to analyze and model the relationship between particles and plankton compositions (multivariate data cloud built by logarithm of the concentrations of particular size fractions, described by a resemblance matrix) and explanatory variables that were divided into three groups: i) spatial (depth and horizontal location), ii) environmental (temperature, salinity, chlorophyll), and iii) size (vertical extension and area). In all models, the forward selection procedure was used to determine the best combination of predictor variables, for explaining variation in particles and plankton size-fractionated composition. DistLM does a partitioning of variation in a data cloud described by a resemblance matrix according to a multiple regression model. It formally fits a linear model of the predictor (environmental) variables to the response (species/size fractions) data cloud, in the space defined by the chosen resemblance measure that define the shape and structure of the data cloud. In DistLM a direct quantitative partitioning of the multivariate variability that is explained by each of several environmental variables is estimated. Thus, it is possible to determine how much of the variability is attributable to individual predictor variables (either acting alone or in pre-defined sets), and it can be determined explicitly how much overlap there is in this explained variation. For this reason, a forward selection was chosen, in which the predictor variable with the best value for the selection criterion is chosen first, followed by the variable that, together with the first, improves the selection criterion the most, and so on. Forward selection therefore adds one variable at a time to the model, choosing the variable at each step which results in the greatest improvement in the value of the selection criterion. At each step, the conditional test associated with adding that variable to the model is also done. The procedure stops when there is no further possible improvement in the selection criterion (Anderson et al., 2008). The relationship between patterns in a resemblance matrix and a set of predictor variables (such as environmental variables) can be observed directly using a constrained ordination: distance-based redundancy analysis (dbRDA). In the dbRDA routine, the structure of the data cloud is viewed through the eyes of the model, where the location of points are the centroids of data clouds of specific patches and the lines/arrows indicate a direction of their relation with specific predictor variables. The amount (percentage) of variation that was explained by each particular group of the factors were schematically plotted as the proportional size of the bars (when all the factors were included in one model) and dots (when the groups of factors were tested in separate models).

Map of the study area was prepared with the PlotSvalbard package in R, created by Vihtakari (2019). Section plots of the

distribution patterns were prepared in the Ocean Data view software, with the application of Diva interpolation (Schlitzer, R.; 2018. Ocean Data View, https://odv.awi.de). The other plots were made in R *via* the "ggplot2" package.

Results

Distribution patterns

In KONG, the cores of the warmest water (8°C) were localized far offshore and were distributed vertically even up to 40 and 50 m depth in 2014 and 2017, respectively (Figure 2). Such a high seawater temperature was observed in the upper 20 m layer over most of the transect in 2019 and inside the fjord in 2015 and 2016. A strong signal of cold (< 5°C) and fresh (salinity <30) glacial meltwaters was observed in the surface 10-m layer of the innermost parts of the fjord each year, but with a degree of variability, i.e., stronger impact in 2015, 2016, 2018 and weaker in 2014, 2017, 2019. The higher chlorophyll fluorescence was observed in the middle of the transect in 2019 and further offshore in 2017 (Figure 2). In general, the elevated values of chlorophyll fluorescence were concentrated in the middle part of the studied water column (ca. 25 m), but occasionally also deeper (up to 50 m offshore in 2014, in the fjord in 2015 and 2019), or close to the surface (near glacier in 2014, 2015 and 2019, or far offshore in 2019).

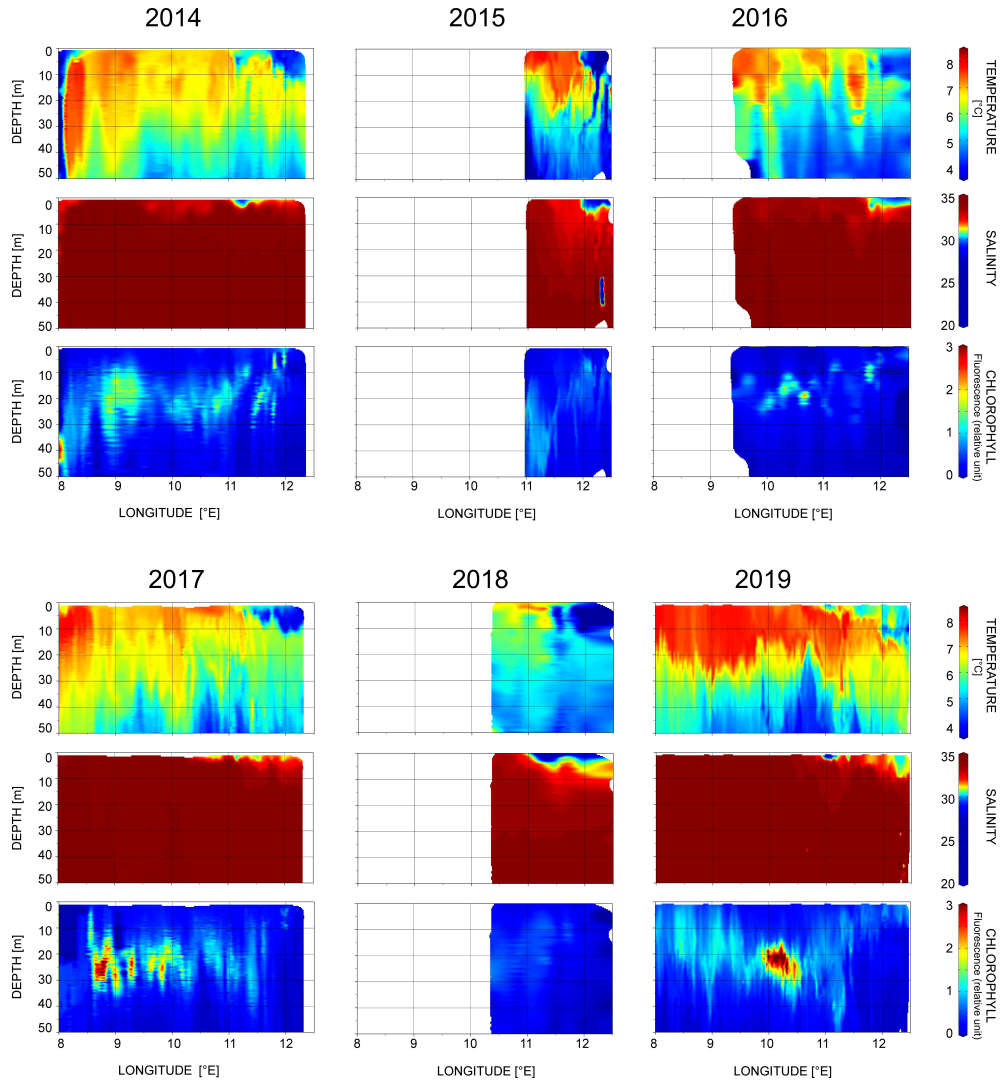

FIGURE 2
The section plots of temperature, salinity and chlorophyll fluorescence distribution in Kongsfjorden over studied summer seasons 2014-2019.

In none of the studied seasons the pattern of hydrographical structure had any obvious reflection on the distribution patterns of particles and plankton (Figure 2 and Supplementary Figures 2, 3). The peaks of chlorophyll fluorescence were associated with concentration hotspots of the Nano, Micro and Small size fractions in 2014 and 2017, and only with the Nano fraction in 2016 and 2019. The Pico fraction was mostly concentrated near surface (upper 5 m) and over wider depth range only close to the glacier front. In the majority of cases very high concentrations of all particle and plankton size fractions were observed at the end of the transect, which was located in the glacial bay (Figure 2 and Supplementary Figures 2, 3). The Medium and Large size fractions were mostly decoupled in space with both chlorophyll fluorescence and other, smaller size fractions, apart from the glacial front parts. A distribution pattern was quite similar between Medium and Large size fractions in most investigated seasons, but totally different in 2015 and 2019, when Medium fraction was mainly concentrated in the lower, innermost part of the investigated transect, while Large fraction was scattered in form of small but numerous sub-patches in a fjord and its entrance. In 2015 the Large size fraction was the only one which distribution reflected clearly the distribution of chlorophyll fluorescence.

In ISF, the highest seawater temperatures (> 6°C) were recorded in the upper 20 m layer, while the lowest (< 1°C) were observed below 40 m at the end of the transect, near the glacier front (Figure 2 in Szeligowska et al., 2020). Along this transect a shallow submesoscale eddy (approximately a few kilometers of diameter) was observed in 2016, 2017 and 2018. It was associated with a discontinuity of the chlorophyll fluorescence concentration peaks. In general, the fluorescence of chlorophyll was restricted to the upper 20 m layer. Similarly, as in KONG, the hydrographical structuring and distribution pattern of chlorophyll fluorescence peaks had no obvious reflection on the distribution patterns of particles and plankton (Figure 3 in Szeligowska et al., 2020). The high spatial compatibility was observed between Nano, Micro and Small size fractions in 2017 and 2018. The concentrations of all size fractions were much higher in 2018 than in other studied years.

Size spectra over time and space

In most cases a good compatibility between size spectra of LISST and LOPC measurements was observed (Supplementary Figure 4). The small divergence between the concentrations obtained by the two methods (the higher values provided by LISST) within the corresponding size fractions was observed in 2018 in both KONG and ISF.

In KONG, the size spectra slopes differed significantly among years (2-way ANOVA, $F = 27.8$, $p < 0.001$) and sub-regions ($F = 5.0$, $p = 0.001$). Also, the interaction between the factor of Year and Region was statistically significant (F=2.7,

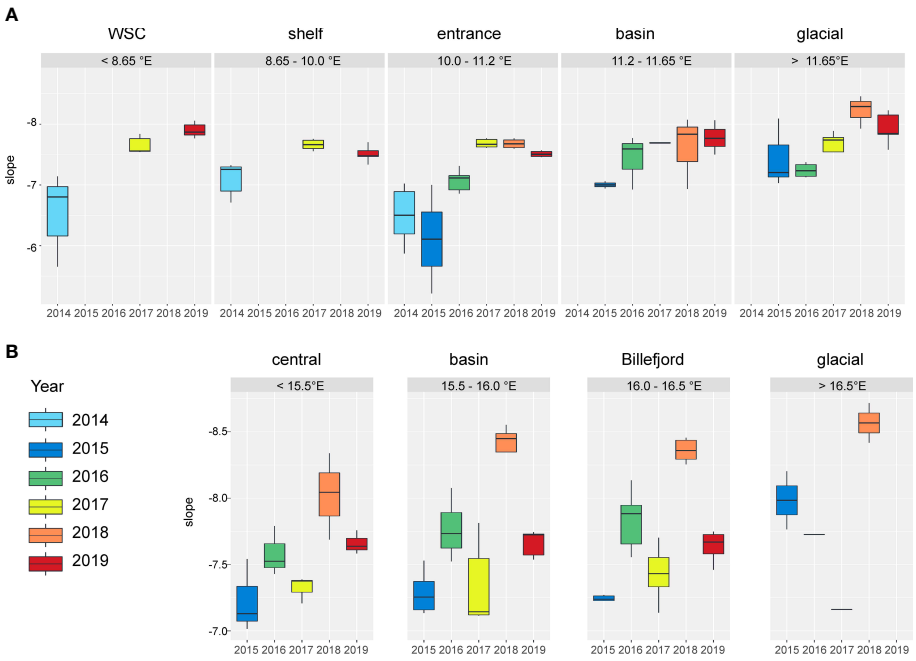

FIGURE 3
The box plots of size spectra slopes over inter-annual and spatial (over longitudinal steps) variability in **(A)** Kongsfjorden and **(B)** Isfjorden.

p=0.004). In general, flatter size spectra slopes were recorded during the first three years of the study and the spectra tended to get steeper over time towards the last studied years (Figure 3A). Especially flat size spectra slopes (>-7) were recorded furthermost offshore in 2014 and in the fjord's entrance in 2014 and 2015. The steepest particles and plankton size spectra (<-7.5) were recorded inside the fjord in 2018 and 2019.

In ISF, the size spectra slopes differed significantly among years (2-way ANOVA, $F = 64.67$, $p < 0.001$), only slightly among sub-regions ($F = 5.46$, $p = 0.002$), but the interaction between the factor of Year and Region was not statistically significant (F=2.1, p=0.037). Flatter size spectra slopes were recorded in 2015 and 2017. The trend of spectra getting steeper over time was observed over 2015-2016-2018 and 2017-2019 (Figure 3B). The steepest particles and plankton size spectra were recorded in 2018 (mean: -8.5).

Patch characteristics

Overall 94 patches were distinguished. The data points assigned as patches represented the minority of the studied space (the overall mean 12%) (Table 1). In KONG, patches occupied slightly smaller fraction of data points, ranging from 1 to 22% (12% mean), while in ISF patches occupied from 5 to 25% (13% mean) of data points. Because of the extremely high concentrations of particles and plankton near glacier front in KONG in 2015 and 2018, only very few data points of the three smallest size fractions were assigned there as 'patches' (Table 1).

On average, the concentrations within patches exceeded the background (mean + sd) by a factor of 1.6 (Supplementary Table 2). This was on average 1.8 in KONG and 1.5 in ISF for the three smallest size fractions and 1.5 in KONG and 1.4 in ISF for the three larger size fractions. The highest observed ratio (4.1) was found in the patch of the Pico fraction found in KONG near glacier in 2018.

The distinguished patches ranged in horizontal length from 1 to 92 km, with median value of 12,8 km in KONG and 11,4 km in ISF and vertically ranged from 5 to 50 meters, with 27 m median in KONG and 23 m in ISF (Supplementary Table 2). The horizontal extension of the patches was the smallest for the Micro, Small and Medium size fractions (<15 km), and the largest for the Nano and Pico fractions (Figure 4). The vertical extension of the patches increased with size from Pico (12 m on average) towards the Small fraction (47 m on average). Then, a decreasing trend through Medium (35 m on average) towards Large (21 mon average) size fraction was observed (Figure 4). The variations between the vertical and horizontal extensions resulted in a similar size (area) of the patches across size fractions, with generally slightly larger spatial coverage of the Nano and Small fractions.

The highest ratio between the variance and mean concentrations and thus the highest values of indices of spatial heterogeneity (Lloyd's patchiness and crowding indexes) were observed in the patches of the Pico size fraction. Then the values of all the indices clearly decreased with size, with the lowest ranges for the Large size fraction (Figure 4). The largest difference (decreasing step) was observed between the Nano and Micro size fractions, whereas only subtle decreasing trend was observed between the larger size fractions (Small, Medium, Large).

Co-occurrence of patches

In KONG, the most frequent recurring pattern of patches localization was observed in the innermost part of the transect (Figure 5), which resulted in the multi-size-fraction patches. The co-occurrence of the patches of four fractions (from Pico to Medium) was observed in 2015, 2016, and 2019. In 2018 all five size fractions had their concentration hotspots in the glacial bay of KONG, but with an interesting size-dependent

TABLE 1 Percentage of the data points representing patches of particular size fractions in subsequent summer seasons.

	Size fraction	2014	2015	2016	2017	2018	2019
Kongsfjorden	Pico	15	1	12	6	2	6
	Nano	16	2	7	18	4	13
	Micro	15	2	10	11	5	7
	Small	12	18	13	21	22	9
	Medium	20	8	8	19	17	5
	Large	10	12	8	15	14	9
Isfjorden	Pico		12	13	16	5	8
	Nano		13	17	21	14	25
	Micro		8	10	13	18	5
	Small		11	10	17	21	9
	Medium		7	8	11	15	10
	Large		11	9	14	14	13

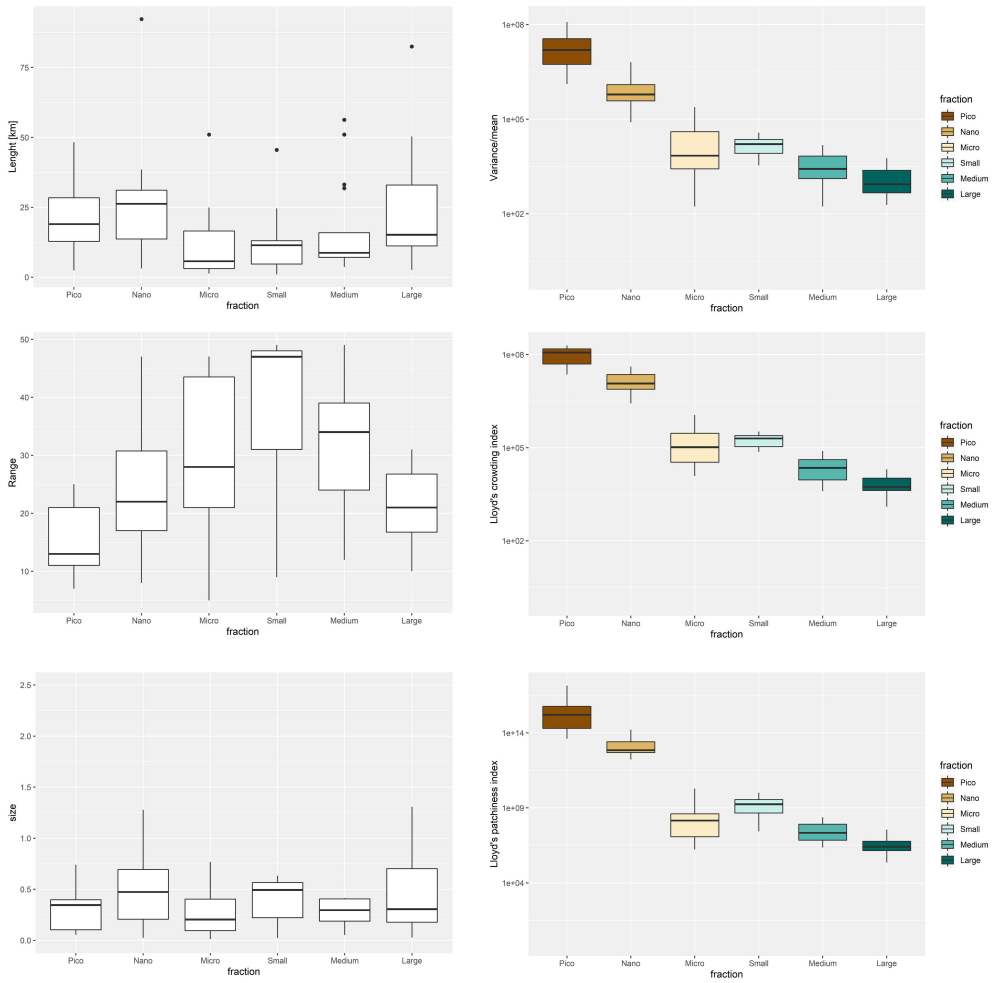

FIGURE 4
Box plots of the horizontal length (km), depth Range (m) and area of size fractionated patches together with indices of spatial heterogeneity.

pattern that smaller fractions (Pico, Nano) concentrated near the surface, intermediate fractions (Micro, Small) slightly deeper, and the two largest fractions (Medium, Large) concentrated in the lowest parts of the studied water column. A similar to same degree tendency was observed also in 2016 and 2019 (with the exception of the Large size fraction). In general, in many cases the patches occupying the innermost parts of the transect extended vertically over wide depth ranges.

The co-occurrence of the patches localized out of the KONG (the first part of the transect) was spectacular in 2014 and 2017, spanning between Nano to Large fractions (Figure 5). Additionally, in 2014 similar huge patches of Medium and Large fractions were observed inside the fjord. The Large size fraction had the most individual distribution patterns in the sense that its patches had often different locations than the other size fractions.

In ISF, where the spatial coverage of the transect was smaller, the occurrence of multi-size-fraction patches was even more frequent than in KONG. Mainly the extensive surface patches of the Pico and Nano fractions were observed over all studied years (Figure 6). In 2016 this pattern was continued by also larger size fractions (Micro, Small and Medium) resulting in large multi-size-fraction patch. The Nano fraction also often co-occurred with similar patches of the Micro fraction (e.g., 2015, 2018). The interesting multi-size-fractioning of the patch was observed in 2017, starting from the deepening middle parts the large Pico and Nano patches, which was repeated by the Micro fraction at only middle part of the studied upper 50 m layer, which in turn was reflected by the high concertation of the Small and Medium fractions at the same location, at the deepest parts of the studied layer (Figure 6). Such a case of a vertically deepening position from the smaller towards larger size fractions was also observed in 2015 and twice in 2018.

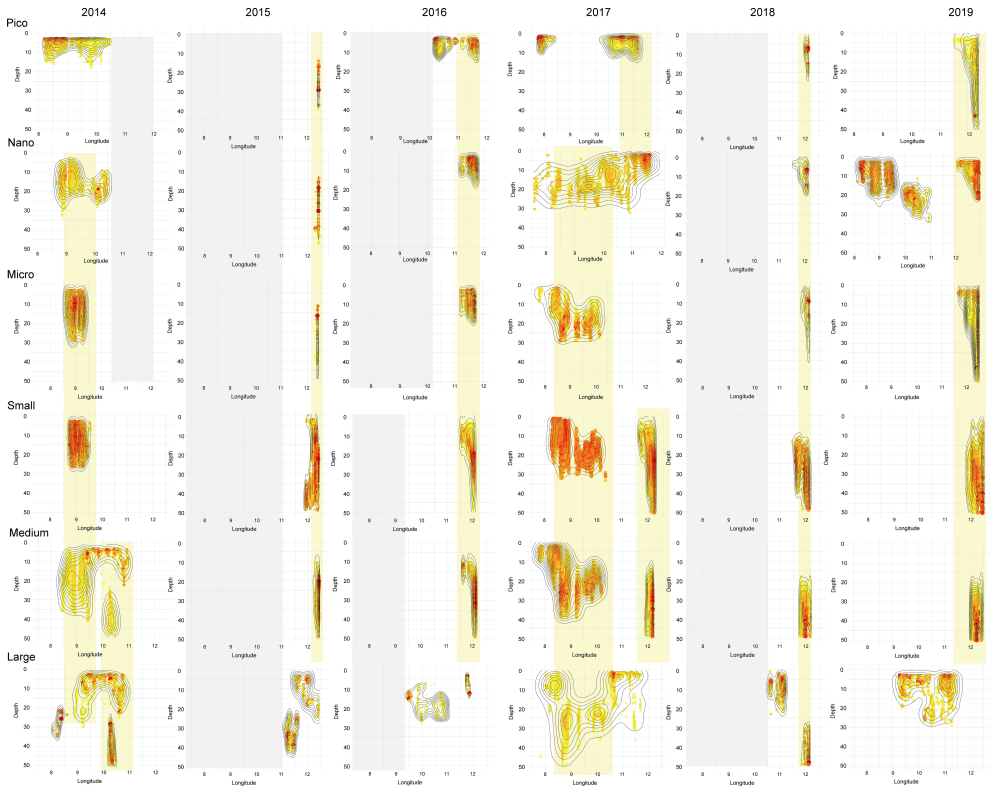

FIGURE 5
The location and internal structure of patches of particular size fractions (rows) over studied years (columns) in Kongsfjorden. The colors and sizes of dots represent the concentrations (scales independent for each patch are presented at Supplementary Figure 5). The black contours indicate the density of concentrations (function stat_density_2d). The grey shadow indicates no data. The yellow frames indicate the co-occurrence of patches of various size fractions.

Typology of patches

When analyzing particular patches, it was evident that they differ significantly in their shapes and structure, depending on their density core location (Figures 5, 6). In consequence, 7 functional types of patches were distinguished: Belt, Triangle, Diamond, Flare, Fingers, Flag, and Rosette (Figure 7). The most common shapes of the designated patches were Flare (19%) and Triangle (18%) types (Supplementary Table 2). Belt and Diamond (15% of patches each) were the second dominant types. Belt and Flag (12% of patches) were mostly observed in the innermost parts of both transects. Many patches (34%) had their cores in the central parts [especially Diamond and Rosette (11% of all patches) types] (Figure 7). In other cases, they had their cores near surface (23% with upper corner and 15% with upper border), occasionally also at the bottom of the patch (9 cases), or did not have any obvious center of aggregation (15 cases) (Supplementary Table 2). In general, the types of patches were not specific to region nor size fraction, because each patch type occurred in each region and was exposed by each size fractions (Figure 7). The long vertically types (Belt and Flag) were a little bit more common in the innermost parts of the fjords. Large size fraction frequently aggregated in form of Flare or Triangle. Triangle was also a common shape built by the Pico fraction. Flag and Rosette shapes were observed mostly as the Small fraction aggregations (Figure 7).

What correlates with patches?

In KONG, seawater temperature and chlorophyll correlated negatively with concentrations of all size fractions except the Large one (Supplementary Figure 5). Low salinity was favorable only for the Pico, Nano and Micro size fractions. Higher water temperature, salinity and chlorophyll enhanced the formation of the larger patches (significant positive correlations with their size), but with lower indices of spatial variability. In ISF, a different pattern of significant correlations between patch parameters was observed, with almost no correlations found with spatial heterogeneity indices and only few significant relations with environmental settings [e.g., Micro, Small and Medium size fractions correlated negatively with water temperature and chlorophyll, whereas the Pico and Large size fractions correlated negatively with salinity and positively with chlorophyll (Supplementary Figure 5)].

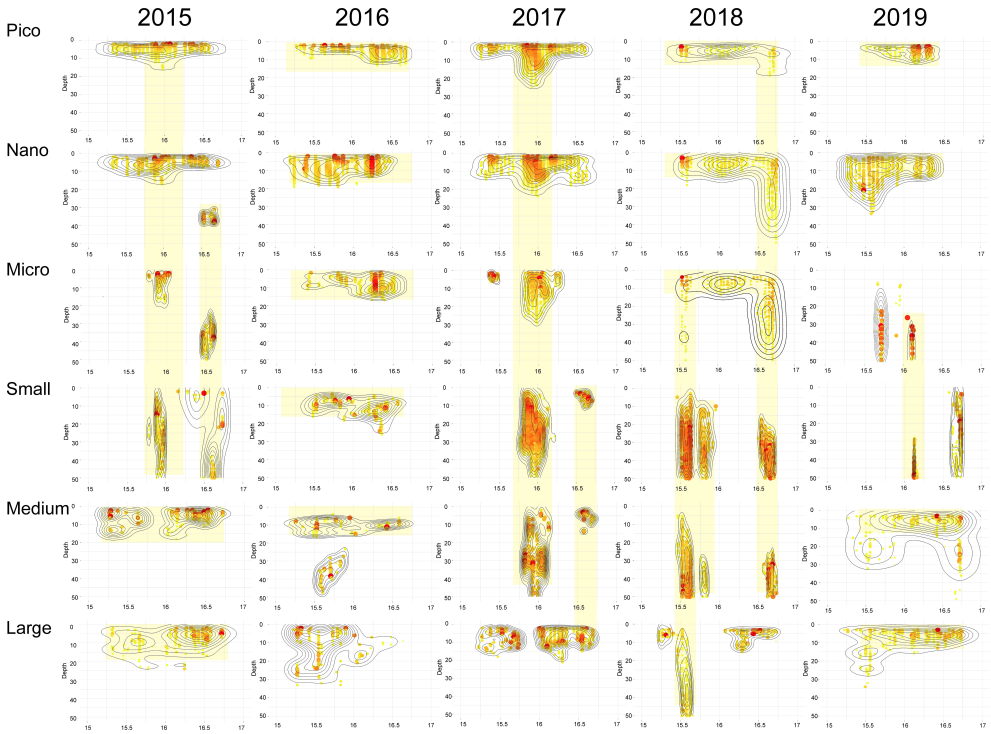

FIGURE 6
The location and internal structure of patches of particular size fractions (rows) over studied years (columns) in Isfjorden. The colors and sizes of dots represent the concentrations (scales independent for each patch are presented at Supplementary Figure 6). The black contours indicate the density of concentrations (function stat_density_2d). The yellow frames indicate the co-occurrence of patches of various size fractions.

In both regions, approximately half of the variation in size-fractionated particle and plankton concentrations in all the distinguished patches was explained in a DistLM model by the studied patch characteristics (51% in KONG and 45% in ISF) (Figure 8 and Supplementary Table 3). In KONG, the most important factor in the DistLM model of all the explanatory variables considered together, was location of the patch (34% of variation). Therefore, a dbRDA scaling showed that in KONG the

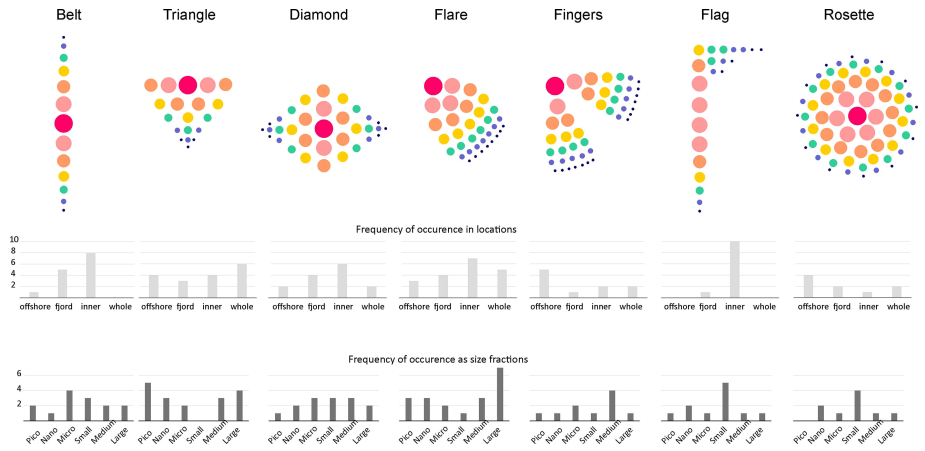

FIGURE 7
Schemes of the proposed types of patches basing on their shape, structure and the location of the Kernel density. Bars: frequency of occurrence in various locations and over size fractions.

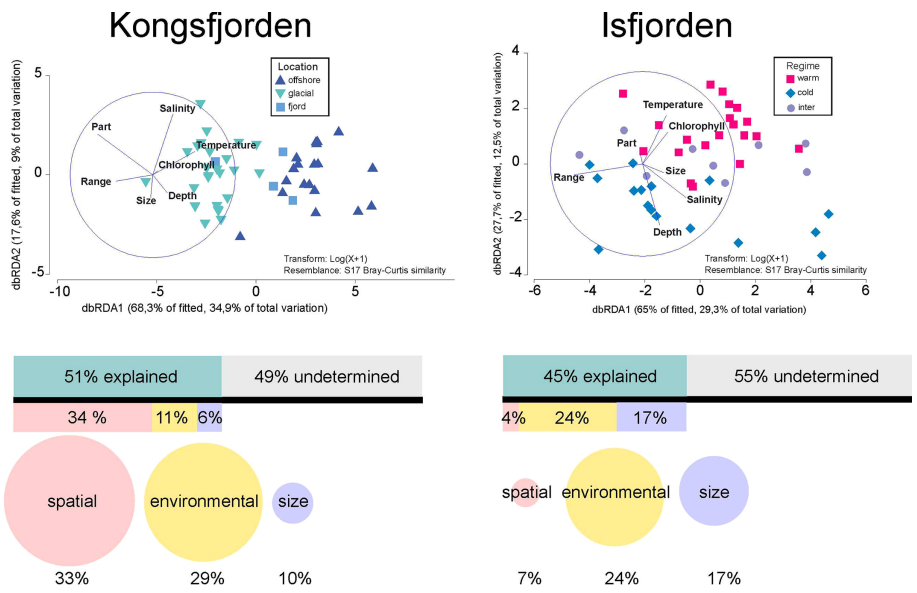

FIGURE 8
Distance-based Redundancy analysis (dbRDA graphs) presenting the relations between the multidimensional scaling of the particles and plankton composition in patches (centroids presented by color-coded markers) and explanatory factors (vectors) in two studied regions. Results of the DistLM model (direct percentage partitioning of the multivariate variability in composition of patches explained by each of several environmental variables) are presented as bars and circles. The bars indicate the percentages explained, when all explanatory variables were considered together. The size of the circles indicates their roles in separate analyses, where groups of factors [the spatial patch locations (vertical and horizontal coordinates of patch presence), environmental settings (temperature, salinity, chlorophyll), and size of the patch (vertical range and area)] were tested in independent DistLM models.

patches located offshore scaled positively with higher water temperature and chlorophyll fluorescence, while the similar types of patches were located in glacial bays (scaled with the same position – Part of the transect) and had a wide vertical range (Figure 8). Whereas in ISF the environmental variables explained the highest amount of the observed variation (21%), and a dbRDA scaling showed that the patches located in warm waters scaled positively with higher chlorophyll fluorescence, while patches located in cold regimes scaled positively with salinity and were located in lower parts of the studied water column (Figure 8). However, when running the separate DistLM models for the individual sets of the parameters, it turned out that in KONG the environmental variables explained almost the same percent of the observed variation (29%) as spatial constraints (33%) (Figure 8).

Discussion

Did the distribution of particles and plankton patches differ over time and space?

Regardless of the considered size fraction and the studied fjord system, the distribution patterns of particles and plankton patches was not repeatable in subsequent years on the same locations of transects, except for the permanently greater particles accumulation at glacier fronts (Supplementary Figures 2, 3; Figures 5, 6). This regularity in concentration hot posts could be a results of increased biological production due to an additional supply of nutrients by tidewater glaciers (Halbach et al., 2019; McGovern et al., 2020) and/or increased discharge and flocculation of particles (Trudnowska et al., 2014; Szeligowska et al., 2020; Szeligowska et al., 2021). In general, the observed distribution patterns of plankton and particles did not clearly reflect the patterns of the environmental water structuring (Figure 2). This relation existed but was rather weak, as the considered environmental cues (temperature, salinity, chlorophyll), explained only 20-30% of overall studied variation (Figure 8; Supplementary Table 3). However, the development and persistence of the observed patches were occasionally related to the occurrence of glacier impact, eddy, sea mountain and hot spots of chlorophyll fluorescence. Because the considered patches contained various components: co-existing living and non-living particles and plankton that could also differ compositionally over time and space, the high variability in observed patterns of patchiness provides a wide spectrum of possible factors and causes of their formation to be considered and discussed.

The factors that could play an important role in structuring a distribution of particles and plankton

Because the physical processes act naturally at different spatial and time scales than plankton growth and activity

(Prairie et al., 2012; Mahadevan, 2016), they mostly shape patches at large scale, while the relative importance of the biotic processes increases inversely with scale (Pinel-Alloul, 1995). Therefore it is important to realize which processes operate on local and which on oceanic scales when trying to decipher patterns in particles and plankton distributions (Prairie et al., 2012; Kuhn et al., 2019). In the case of the patches analyzed in this study, the local environmental variables were the most crucial in the case of the fjord, where smaller spatial scale was investigated (ISF), whereas the large scale spatial effect was privileged when the larger distance, including offshore area, and thus wider spectrum of environments was considered (KONG) (Figure 8; Supplementary Table 3). As both fjords are opened and prone to intensive Atlantic water advection (Figure 1), which definitely re-shapes plankton communities (Basedow et al., 2004; Kubiszyn et al., 2014; Skogseth et al., 2020; Trudnowska et al., 2020b), mostly in favor of smaller species, the high importance of this large scale oceanic circulation has to be credited. Whereas melting glaciers were clearly recognized as the dominating local process, causing high particles and plankton accumulations in the innermost glacial bays (Figures 5, 6), which is typical for the summer melting period (Meire et al., 2017; D'Angelo et al., 2018; Kanna et al., 2018; Szeligowska et al., 2020; Trudnowska et al., 2020a). Therefore, the fact that a distribution of particles and plankton was not strictly reflecting the hydrographical structuring implies that they are not just purely dye-like passive tracers of advection, freshwater run off and/or local stratification of the water column, but there must have existed also some other factors that enhance their accumulation, most probably of ecological origin. Possible drivers include evolving nutrient-light availability, spatial and temporal changes in respiration and production along the effect of submesoscale upwelling or downwelling processes (Stanley et al., 2017).

Since the summertime in the Arctic is a time of intense biological production and plankton activity (Trudnowska et al., 2014; Kubiszyn et al., 2017; Svensen et al., 2019), the local seasonal dynamics of their blooms must have also played an important, albeit inestimable, role in shaping the observed patchy distribution patterns and high concentrations of plankton. The biological factors could only be represented by the chlorophyll fluorescence levels and cross-correlations among size fractions (Supplementary Figure 5). Indeed, sometimes large multi-size-fraction patches matched the peaks of chlorophyll fluorescence (Figures 5, 6 vs. Figure 2). But more generally neither the distribution patterns nor the concentrations of most of the size fractions correlated significantly with chlorophyll, which suggests that some of those concentration hotspots did not consist of actively fluorescent particles or plankton. The significant correlation got for the Large size fraction in ISF (Supplementary Figure 5) could indicate either the fluorescent nature of marine aggregates (Timmerman et al., 2014; Graff and Menden-Deuer, 2016; McManus et al., 2021), or the spatial match between herbivorous grazers [as the Large fraction is mostly represented by *Calanus* copepods (Balazy et al., 2018; Balazy et al., 2019)] and food stocks (expressed as high chlorophyll levels).

A trend of an increasing role of the smallest size fractions expressed in this study as steepening size spectra slopes over years (Figure 3) was consistent in the two studied regions, at least until 2018. The steep size spectra slopes correlated with the abundance of Pico, Nano and Micro size fractions and the 'crowding' indexes in both regions, while in KONG it was also slightly positively correlated with seawater temperature and chlorophyll fluorescence, probably due to higher primary production building steep size spectra slopes. A shift in plankton size structure towards the proliferating importance of small size fractions, particularly a Pico fraction, is now a widely recognized effect of the progressing climate warming in the Arctic (Li et al., 2009; Nöthig et al., 2015; Metfies et al., 2016), related to the increased advection of Atlantic waters. Meanwhile, the steepest size spectra slopes observed in 2018 could be related also to some other mechanisms: e.g., the resuspension of sediments, disaggregation of marine aggregates due to the stormy weather, blooms of *Phaeocystis pouchetii*, or high concentrations of copepods nauplii, as observed in Isfjorden (Szeligowska et al., 2020), which in fact are also manifestations of observed currently changes in the Arctic epipelagial. The spatial and inter-annual variability in size spectra of distinguished patches (Figure 3) could also have resulted from different productivity states of the pelagic communities, driven by the shifts in dominating species. For example, the spatial switch in relative roles between Pico and Nano fractions in KONG in 2017 was explained by the preference of the Pico fraction species for regenerated nitrogen, while a higher proportion of the species representing Nano fraction was observed in the relatively cold and turbid surface water in the inner basin (Kim et al., 2020). Observed differences in size structure could also reflect differences in plankton phenology, as a result of e.g., the seasonal succession from larger diatoms to smaller dinoflagellates, meroplankton blooms, or different developmental stage composition of the dominating copepods (White et al., 2015; Balazy et al., 2019; Szeligowska et al., 2020; Balazy et al., 2021).

The observed higher variability in particle and plankton size distribution over time than over space (Figure 3) was indicated also by others (Jouon et al., 2008; D'Angelo et al., 2018; Szeligowska et al., 2020), which suggests that particles remain similar over relatively extensive spatial scales, but differentiate with years and/or seasons.

What was the spatial scale of particles and plankton patchiness?

The patches occupied the minor part of the studied water column (on average 12%, ranging from several percentages up to

25%, Table 1), which is generally similar to the ones observed on the west Spitsbergen shelf [2-17%, (Trudnowska et al., 2016)], and in East Sound fjord in USA (12% (Menden-Deuer, 2012), but much less than observed in St. Lawrence Estuary in Canada (80% (Currie et al., 1998). The concentrations within patches were on average only 1.6 times greater than the background concentrations (Supplementary Table 2), which is less than in previous studies [e.g. 2.5 to 5.1 (Wiebe, 1970), 2.7-17.5 (Trudnowska et al., 2016)]. However, occasionally the concentrations were much greater (4.1, 2.7, 2.6), especially for the Pico fraction (Supplementary Table 2).

The majority of the patches distinguished in this study were longer than 10 km (Supplementary Table 2), which agrees with the ranges presented in the most recent study of the wide spectrum of plankton patchiness (Robinson et al., 2021). However, those authors concluded that longer sampling transects (50 to 100 km) are needed to elucidate the true patch length for copepods and phytoplankton groups. The results of this study showed that only 6 out of the 94 studied patches exceeded horizontally 50 km, 9 exceeded 40 km, and 21 patches were longer than 20 km (Supplementary Table 2). Despite the fact that this study was restricted to the upper 50-meters, the vertical extension of most of the detected patches (26 m) exceeds considerably the limit (several meters) for thin plankton layers (Dekshenieks et al., 2001; McManus et al., 2005; Benoit-Bird et al., 2013) and greatly ranks to the ranges (10-30 m) recently observed for the 36 plankton taxa (Robinson et al., 2021).

Generally, the length of patches was inversely related to organisms' size, as the extension of the patches of the smaller size fractions was frequently much wider than the extension of the larger fractions (Supplementary Table 2; Figures 5, 6), which agrees with the rule that dispersal scales show a negative correlation with body size (Villarino et al., 2018; Robinson et al., 2021). Also, a clear negative trend between size fraction and all the applied indices of spatial heterogeneity was observed (Figure 4; Supplementary Figure 5) in form of the higher the crowding/patchiness index for smaller fractions (Supplementary Table 2), implying that not only the spatial extension is wider for smaller fractions, but also their gathering rates are greater. This in turn could be explained by the mechanisms that after the inflection point of the density the smaller patches begin to merge to larger (but fewer) patches (Robinson et al., 2021).

Were the patches of various size fractions of particles and plankton co-occurring?

The spatial compatibility of distribution patterns of various size fractions resulted in a generation of multi-size-fraction form of patches. Because of the high degree of variability in the combinations of pairs/groups of co-occurring size fractions, it is really difficult to bring more specific conclusions. It just can be summarized that under some conditions there were in force mechanisms favorable for a specific set of particles or plankton fractions to gather together, but absolutely neutral or unfavorable for other fractions which in turned gathered together under other conditions.

The occurrence of the large multi-size-fraction patches observed on the west Spitsbergen shelf of KONG (2014, 2017) was associated with the elevated concentrations of chlorophyll fluorescence (Figures 5 vs. Figure 2), which points towards the ecological hypothesis, e.g. a mechanism of gathering in the concentration hotspots of the potential prey (Holliday et al., 2003). Studies of spatial overlap between individuals typically assume that shared habitat must result in interaction (Carroll et al., 2019; Greer et al., 2021), which is probably especially true in the case of the pairs of fractions (e.g., Medium & Large in 2014 in KONG, Figure 5). The most interesting feature of the observed multi-size-fraction patches was their exact horizontal compatibility, but with shifts their vertical position in vertical plane. Intuitively it can be interpreted as an effect of different rates of sedimentation, with larger particles descending quicker (deeper concentrations) and smaller ones floating over longer time in the uppermost layers (Stemmann and Boss, 2012; Giering et al., 2020). Whereas the occurrence of such interesting, vertically portioned multi-size-fraction patch in a middle of the ISF in 2017 (Figure 6) resulted most probably from the eddy formation (Szeligowska et al., 2020). Here, similarly as in a case of previous study reporting the spatial relation between eddy and distribution of size fractionated plankton (Trudnowska et al., 2016), the concentrations were higher on the edges of an eddy than inside the eddy. Most of the multi-size-fraction patches were observed in glacial bays (Figures 5, 6), where water is constantly highly loaded by mineral particles, marine aggregates and local populations of plankton (Trudnowska et al., 2014; Meire et al., 2017; D'Angelo et al., 2018; Kanna et al., 2018; Halbach et al., 2019; Szeligowska et al., 2020; Trudnowska et al., 2020a).

Inferring about the composition of particles and plankton

As shown by the very first studies of patchiness, the abundance patch does not necessarily coincide with its taxonomical homogeneity, as it may be formed by a bloom of a specific species or a group of species (Mackas, 1984), resulting in compositionally heterogeneous patches (Greer et al., 2016). The same applies to a variety of possible compositions of marine particles. The structural differences of the patches designated in this study (Figure 7) could only be speculated basing on variations in size spectra of particles and plankton within the patches, and our general ecological knowledge of the plankton

composition observed during summer in studied regions. Typically dinoflagellates (Bhaskar et al., 2020) or diatoms (Piwosz et al., 2009) dominate the summer community structures of protists in Kongsfjorden, while *Phaeocystis pouchetii* dominate in Isfjorden (Kubiszyn et al., 2017), together with Cryptophytes and Ciliates (Szeligowska et al., 2020). Zooplankton in turn is mainly dominated in both fjords by two size fractions of copepods, such as *Oithona* (Small to Medium fraction) and *Calanus* – the main representative of the Large size fraction (Gluchowska et al., 2016; Hop and Wiencke, 2019; Szeligowska et al., 2020; Trudnowska et al., 2020b). However, the planktonic dominants representing the particular size fractions may vary in both studied regions depending on the year, season, and part of the fjord due to strong horizontal hydro-ecological gradients.

Phytoplankton patches are expected to be more monospecific than zooplankton ones (Mackas, 1984). Also the spatial patterns are different between patches of phytoplankton and zooplankton (Mackas et al., 1985), and between different size classes of those (Trudnowska et al., 2016; Kuhn et al., 2019), which may explain why specific distribution patterns of various size fractions (e.g. the Pico fraction displayed wide horizontal distribution at surface, whereas the Micro and Small fraction patches extended frequently over wide vertical ranges, but with much smaller horizontal range) were observed (Figures 5, 6). However, the fact that Pico fraction was mostly confined to the upper few meters may also be partly an artefact, as the detection of lowest size fractions are sensitive to deviations caused by stray light but also by shape effect, or by the signal produced by the presence of particles smaller than the optical measurement range, which may produce an artificial rising edge (Agrawal et al., 2008; Reynolds et al., 2010; Andrews et al., 2011).

Did the internal structure of particles and plankton patches differ?

So far the portrayal of the patches has mostly been limited to the information about the particles or plankton concentrations and spatial extension of those hot spots (Pinel-Alloul, 1995; Brentnall et al., 2003; Greer et al., 2016; Trudnowska et al., 2016; Robinson et al., 2021), and assumed a circular patch structure to calculate patch area and other properties (Wiebe, 1970; Currie et al., 1998). Hence, so far, the knowledge about the internal structure of the patches is fairly limited and ecologists tend to perceive patches in a simplistic way. The results of this study broaden, but also complicate the perception of the patchiness phenomenon even further by pointing out that the patches can exhibit various internal structuring, resulting in their different shapes (Figure 7).

Inspired by the comment that patches observed at a given spatial resolution may, on examination at a higher resolution, be seen to be patchy themselves (Pinel-Alloul, 1995), we analyzed each patch individually, by focusing on the isolated patches and 'mapping' their internal structures (Figures 5, 6). Even though previous observations imply that plankton is totally randomly distributed within patches (Currie et al., 1998), in most cases the core (kernel density) of particular patches could be depicted. Consequently, a novel classification of patches, depending on their shape and the location of their cores (either in the central part, in the corner or at the border) has been proposed (Figure 7). However, the expectation that particular types will be more frequent in specific locations (with different physical and biological sets of mechanisms) or for specific size fractions (different compositions) has not been proved by this material (Figure 7).

Even though no clear trends between the types of the patches and the studied environmental parameters emerged, it is still appealing to speculate about the causes of their formation, as this may assist reasoning about their origin, fate, role, or functionality. The interesting spectrum of the observed shapes of the particles and plankton patches may be the result of both the active gathering types of the planktonic organisms (e.g., Rosette, Diamond, Triangle, Flare), by the hydrographical structuring (e.g., Belt, Flag), or the irregularities in the water velocity, which might stretch/squeeze, twist and distort them in many various ways (e.g., Fingers) (Mackas et al., 1985). While the horizontal thin layers (up to few meters thickness and horizontal extensions overs many kilometers) are among the best studied patchy forms (McManus et al., 2005; Stacey et al., 2007), typically containing densities far greater than those above or below this layer (Dekshenieks et al., 2001; Durham and Stocker, 2012), the observed in this study thin vertical layers (narrow horizontally, but vertically extended over the studied water column depth range, such as Belt and Flag types), are something not reported so far. Here, they were mostly specific to the glacier fronts, but as they also occurred sporadically in other locations (Medium and Large fraction at the entrance to KONG in 2014 (Figure 5), patches of Micro, Small, Medium and Large in 2018 in ISF (Figure 6) above the tip of seamount), it can be assumed that such structuring may also occur under the impact of other conditions.

How this study integrates and advances the current knowledge

The patchy distribution of particles and plankton is a derivative of a complex set of multi-stage and multi-dimensional processes. At each step of their residence in a given parcel of the water several agents, representing the physical and biological forces, are acting simultaneously (Pinel-Alloul, 1995; Martin, 2003) and the interactions among them often result in an synergistic effect (Levin and

Segel, 1976; Borcard et al., 1992; Borcard and Legendre, 2002), seriously complicating our understanding of their distribution patters. Even though 94 patches of various size fractions of particles and plankton that existed in comparable environmental conditions (two Arctic fjords) over several years of the study were examined thoroughly, it still remains an ambiguous matter when, why, and which of the mechanisms (physical vs. biological vs. chemical) prevails in shaping the patterns of their distribution. The observation that particles and plankton organisms are variously organized in space, both in the ocean and within their individual aggregations, opens a new perspective for studies of the patchiness phenomenon. Thus, this study might indicate a new direction in examining patchiness of plankton and particles by providing a background information on relatively simple shape classification of the detected types of those 'cells of matter and life' as a potentially additional aspect to be considered for understanding e.g., patchiness main drivers, the scale of the coexistence of various size fractions in the same patch space, predator-prey interactions and niche portioning.

Data availability statement

The datasets generated for this study are available on request to the corresponding author.

Author contributions

ET, conceptualization, data curation, formal analysis, investigation, methodology, software, visualization, and writing original draft. KD-D and SS, data curation and editing manuscript draft. KB-S, funding acquisition, project administration, and editing manuscript draft. All authors contributed to the article and approved the submitted version.

Funding

This study was founded by the National Science Centre (Narodowe Centrum Nauki) as PicMac project no. 2013/09/B/NZ8/03365 & CoastDark project no 2018/29/B/NZ8/02463.

Acknowledgments

A previous version of this manuscript appears online as a preprint at Biogeosciences Discussions: https://bg.copernicus.org/preprints/bg-2021-98/#discussion.

Conflict of interest

The authors declare that the research was conducted in the absence of any commercial or financial relationships that could be construed as a potential conflict of interest.

Publisher's note

Supplementary material

The Supplementary Material for this article can be found online at: https://www.frontiersin.org/articles/10.3389/fmars.2022.909457/full#supplementary-material

References

Agrawal, Y. C., Whitmire, A., Mikkelsen, O. A., and Pottsmith, H. C. (2008). Light scattering by random shaped particles and consequences on measuring suspended sediments by laser diffraction. *J. Geophys. Res. Ocean* 113 (4), 1–11. doi: 10.1029/2007JC004403

Anderson, M. J., Gorley, R. N., and Clarke, K. R. (2008). *PERMANOVA þ for PRIMER, guid. to softw. stat. methods* (Plymouth, UK: Prim. Ltd.).

Andrews, S. W., Nover, D. M., Reardon, K. E., Reuter, J. E., and Schladow, S. G. (2011). The influence of ambient light intensity on *in situ* laser diffractometers. *Water Resour. Res.* 47 (6), 1–10. doi: 10.1029/2010WR009841

Avila, T. R., de Souza Machado, A. A., and Bianchini, A. (2012). Estimation of zooplankton secondary production in estuarine waters: Comparison between the enzymatic (chitobiase) method and mathematical models using crustaceans. *J. Exp. Mar. Bio. Ecol.* 416–417, 144–152. doi: 10.1016/j.jembe.2012.02.015

Balazy, K., Boehnke, R., Trudnowska, E., Søreide, J. E., and Błachowiak-Samołyk, K. (2021). Phenology of oithona similis demonstrates that ecological flexibility may be a winning trait in the warming Arctic. *Sci. Rep.* 11 (1), 18599. doi: 10.1038/s41598-021-98068-8

Balazy, K., Trudnowska, E., and Błachowiak-Samołyk, K. (2019). Dynamics of calanus copepodite structure during little auks' breeding seasons in two different Svalbard locations. *Water* 11 (7), 1405. doi: 10.3390/w11071405

Balazy, K., Trudnowska, E., Wichorowski, M., and Błachowiak-Samołyk, K. (2018). Large Versus small zooplankton in relation to temperature in the Arctic shelf region. *Polar Res.* 37 (1), 1427409. doi: 10.1080/17518369.2018.1427409

Barnes, C., Maxwell, D., Reuman, D. C., and Jennings, S. (2010). Global patterns in predator — prey size relationships reveal size dependency of trophic transfer efficiency. *Ecology* 91, 1, 222–232. doi: 10.1890/08-2061.1

Basedow, S. L., Eiane, K., Tverberg, V., and Spindler, M. (2004). Advection of zooplankton in an Arctic fjord (Kongsfjorden, Svalbard). *Estuar. Coast. Shelf Sci.* 60 (1), 113–124. doi: 10.1016/j.ecss.2003.12.004

Benoit-Bird, K. J., Kuletz, K., Heppell, S., Jones, N., and Hoover, B. (2011). Active acoustic examination of the diving behavior of murres foraging on patchy prey. *Mar. Ecol. Prog. Ser.* 443, 217–235. doi: 10.3354/meps09408

Benoit-Bird, K. J., Shroyer, E. L., and McManus, M. A. (2013). A critical scale in plankton aggregations across coastal ecosystems. *Geophys. Res. Lett.* 40 (15), 3968–3974. doi: 10.1002/grl.50747

Bhaskar, J. T., Parli, B. V., and Tripathy, S. C. (2020). Spatial and seasonal variations of dinoflagellates and ciliates in the kongsfjorden, Svalbard. *Mar. Ecol.* 41, 1–12. doi: 10.1111/maec.12588

Blanchard, J. L., Heneghan, R. F., Everett, J. D., Trebilco, R., and Richardson, A. J. (2017). From bacteria to whales: Using functional size spectra to model marine ecosystems. *Trends Ecol. Evol.* 32 (3), 174–186. doi: 10.1016/j.tree.2016.12.003

Borcard, D., and Legendre, P. (2002). All-scale spatial analysis of ecological data by means of principal coordinates of neighbour matrices. *Ecol. Modell.* 153 (1–2), 51–68. doi: 10.1016/S0304-3800(01)00501-4

Borcard, D., Legendre, P., and Drapeau, P. (1992). Partialling out the spatial component of ecological variation author. *Ecology* 73 (3), 1045–1055. doi: 10.2307/1940179

Borja, A., Andersen, J. H., Arvanitidis, C. D., Basset, A., Buhl-Mortensen, L., Carvalho, S., et al. (2020). Past and future grand challenges in marine ecosystem ecology. *Front. Mar. Sci.* 7. doi: 10.3389/fmars.2020.00362

Boudreau, P. R., Dickie, L. M., and Kerr, S. R. (1991). Body-size spectra of production and biomass as system-level indicators of ecological dynamics. *J. Theor. Biol.* 152 (3), 329–339. doi: 10.1016/S0022-5193(05)80198-5

Brentnall, S. J., Richards, K. J., Brindley, J., and Murphy, E. (2003). Plankton patchiness and its effect on larger-scale productivity. *J. Plankton Res.* 25 (2), 121–140. doi: 10.1093/plankt/25.2.121

Briseño-Avena, C., Prairie, J. C., Franks, P. J. S., and Jaffe, J. S. (2020). Comparing vertical distributions of chl- a fluorescence , marine snow , and taxon-specific zooplankton in relation to density using high-resolution optical measurements. *Front. Mar. Sci.* 7. doi: 10.3389/fmars.2020.00602

Carroll, G., Holsman, K. K., Brodie, S., Thorson, J. T., Hazen, E. L., Bograd, S. J, et al (2020). A review of methods for quantifying spatial predator–prey overlap. *Glob. Ecol. Biogeogr.* 28, 1561–1577. doi: 10.1111/geb.12984

Cottier, F. R., Nilsen, F., Skogseth, R., Tverberg, V., Skardhamar, J., and Svendsen, H. (2010). Arctic Fjords: A review of the oceanographic environment and dominant physical processes. *Geol. Soc Spec. Publ.* 344, 35–50. doi: 10.1144/SP344.4

Csapó, H. K., Grabowski, M., and Węsławski, J. M. (2021). Coming home - boreal ecosystem claims Atlantic sector of the Arctic. *Sci. Total Environ.* 771, 144817. doi: 10.1016/j.scitotenv.2020.144817

Currie, W. J. S., Claereboudt, M. R., and Roff, J. C. (1998). Gaps and patches in the ocean: A one-dimensional analysis of planktonic distributions. *Mar. Ecol. Prog. Ser.* 171, 15–21. doi: 10.3354/meps171015

D'Angelo, A., Giglio, F., Miserocchi, S., Sanchez-Vidal, A., Aliani, S., Tesi, T., et al. (2018). Multi-year particle fluxes in kongsfjorden, Svalbard. *Biogeosciences* 15 (17), 5343–5363. doi: 10.5194/bg-15-5343-2018

Davis, C. S., Flierl, G. R., Wiebe, P. H., and Franks, P. J. S. (1991). Micropatchiness, turbulence and recruitment in plankton. *J. Mar. Res.* 49, 109–151. doi: 10.1357/002224091784968602

Davis, C. S., Thwaites, F. T., Gallager, S. M., and Hu, Q. (2005). A three-axis fast-tow digital video plankton recorder for rapid surveys of plankton taxa and hydrography. *Limnol. Oceanogr. Methods* 3 (2), 59–74. doi: 10.4319/lom.2005.3.59

Dekshenieks, M. M., Donaghay, P. L., Sullivan, J. M., Rines, J. E. B., Osborn, T. R., and Twardowski, M. S. (2001). Temporal and spatial occurrence of thin phytoplankton layers in relation to physical processes. *Mar. Ecol. Prog. Ser.* 223, 61–71. doi: 10.3354/meps223061

Durham, W. M., and Stocker, R. (2012). Thin phytoplankton layers: Characteristics, mechanisms, and consequences. *Ann. Rev. Mar. Sci.* 4, 177–207. doi: 10.1146/annurev-marine-120710-100957

Ehn, J. K., Reynolds, R. A., Stramski, D., Doxaran, D., Lansard, B., and Babin, M. (2019). Patterns of suspended particulate matter across the continental margin in the Canadian Beaufort Sea during summer. *Biogeosceinces* 16, 1583–1605. doi: 10.5194/bg-16-1583-2019

Forest, A., Stemmann, L., Picheral, M., Burdorf, L., Robert, D., Fortier, L., et al. (2012). Size distribution of particles and zooplankton across the shelf-basin system in southeast Beaufort Sea: Combined results from an underwater vision profiler and vertical net tows. *Biogeosciences* 9 (4), 1301–1320. doi: 10.5194/bg-9-1301-2012

Franks, P. J. S. (2005). Plankton patchiness, turbulent transport and spatial spectra. *Mar. Ecol. Prog. Ser.* 294, 295–309. doi: 10.3354/meps294295

Genin, A., Jaffe, J. S., Reef, R., Richter, C., and Franks, P. J. S. (2005). Swimming against the flow: A mechanism of zooplankton aggregation. *Science* 308 (5723), 860–862. doi: 10.1126/science.1107834

Geoffroy, M., Cottier, F. R., Berge, J., and Inall, M. E. (2017). AUV-based acoustic observations of the distribution and patchiness of pelagic scattering layers during midnight sun. *ICES J. Mar. Sci.* 74 (9), 2342–2353. doi: 10.1093/icesjms/fsw158

Giering, S., Lou, C., Cavan, E. L., Basedow, S. L., Briggs, N., Burd, A. B., et al. (2020). Sinking organic particles in the ocean — flux estimates from *in situ* optical devices. *Front. Mar. Sci.* 6. doi: 10.3389/fmars.2019.00834

Gluchowska, M., Kwasniewski, S., Prominska, A., Olszewska, A., Goszczko, I., Falk-Petersen, S., et al. (2016). Zooplankton in Svalbard fjords on the Atlantic–Arctic boundary. *Polar Biol.* 39 (10), 1785–1802. doi: 10.1007/s00300-016-1991-1

Godø, O. R., Samuelsen, A., Macaulay, G. J., Patel, R., Hjøllo, S. S., Horne, J., et al. (2012). Mesoscale eddies are oases for higher trophic marine life. *PLoS One* 7 (1), 1–9. doi: 10.1371/journal.pone.0030161

Graff, J. R., and Menden-Deuer, S. (2016). Physical and optical properties of phytoplanktonrich layers in a coastal fjord: A step toward prediction and strategic sampling of plankton patchiness. *Mar. Ecol. Prog. Ser.* 544, 1–14. doi: 10.3354/meps11601

Greer, A. T., Cowen, R. K., Guigand, C. M., Mcmanus, M. A., Sevadjian, J. C., and Timmerman, A. H. V. (2013). Relationships between phytoplankton thin layers and the fine-scale vertical distributions of two trophic levels of zooplankton. *J. Plankton Res.* 35 (5), 939–956. doi: 10.1093/plankt/fbt056

Greer, A. T., Woodson, C. B., Smith, C. E., Guigand, C. M., Cowen, R. K., and Koski, M. (2016). Examining mesozooplankton patch structure and its implications for trophic interactions in the northern gulf of Mexico. *J. Plankton Res.* 38 (4), 1115–1134. doi: 10.1093/plankt/fbw033

Greer, A. T., Chiaverano, L. M., Treible, L. M., Briseño-Avena, C., and Hernandez, F. J. (2021). From Spatial Pattern to Ecological Process Through Imaging Zooplankton Interactions. ICES. *J. Mar. Sci* 78 (8), 12664–2674. doi: 10.1093/icesjms/fsab149

Halbach, L., Vihtakari, M., Duarte, P., Everett, A., Granskog, M. A., Hop, H., et al. (2019). Tidewater glaciers and bedrock characteristics control the phytoplankton growth environment in an Arctic fjord. *Front. Mar. Sci.* 6. doi: 10.3389/fmars.2019.00254

Hegseth, E. N., and Tverberg, V. (2013). Effect of Atlantic water inflow on timing of the phytoplankton spring bloom in a high Arctic fjord (Kongsfjorden, Svalbard). *J. Mar. Syst.* 113–114, 94–105. doi: 10.1016/j.jmarsys.2013.01.003

Hodal, H., Falk-Petersen, S., Hop, H., Kristiansen, S., and Reigstad, M. (2012). Spring bloom dynamics in kongsfjorden, Svalbard: Nutrients, phytoplankton, protozoans and primary production. *Polar Biol.* 35 (2), 191–203. doi: 10.1007/s00300-011-1053-7

Holliday, D. V., Donaghay, P. L., Greenlaw, C. F., McGehee, D. E., McManus, M. A., Sullivan, J. M., et al (2003). Advances in defining fine- and micro-scale pattern in marine plankton. *Aquat. Living Res.* 16, 131–136. doi: 10.1016/S0990-7440(03)00023-8

Hop, H., Falk-Petersen, S., Svendsen, H., Kwasniewski, S., Pavlov, V., Pavlova, O., et al. (2006). Physical and biological characteristics of the pelagic system across fram strait to kongsfjorden. *Prog. Oceanogr.* 71 (2–4), 182–231. doi: 10.1016/j.pocean.2006.09.007

Hop, H., Pearson, T., Hegseth, E. N., Kovacs, K. M., Wiencke, C., Kwaśniewski, S., et al. (2002). The marine ecosystem of kongsfjorden, Svalbard. *Polar Res.* 21, 167–208. doi: 10.1016/j.polar.2016.11.001

Hop, H., and Wiencke, C. (2019). *The ecosystem of kongsfjorden, Svalbard*. Springer: Advances in Polar Ecology (AVPE, volume 2)

Jouon, A., Ouillon, S., Douillet, P., Lefebvre, J. P., Fernandez, J. M., Mari, X., et al. (2008). Spatio-temporal variability in suspended particulate matter concentration and the role of aggregation on size distribution in a coral reef lagoon. *Mar. Geol.* 256 (1–4), 36–48. doi: 10.1016/j.margeo.2008.09.008

Kanna, N., Sugiyama, S., Ohashi, Y., Sakakibara, D., Fukamachi, Y., and Nomura, D. (2018). Upwelling of macronutrients and dissolved inorganic carbon by a subglacial freshwater driven plume in bowdoin fjord, northwestern Greenland. *J. Geophys. Res. Biogeosci.* 123 (5), 1666–1682. doi: 10.1029/2017JG004248

Kim, B. K., Joo, M., Jung, J., Lee, B., and Ha, S.-Y. (2020). *In situ* rates of carbon and nitrogen uptake by phytoplankton and the contribution of picophytoplankton in kongsfjorden, Svalbard. *Water* 12, 2903. doi: 10.3390/w12102903

Kotliar, N. B., and Wiens, J. A. (1990). Multiple scales of patchiness and patch structure: A hierarchical framework for the study of heterogeneity. *Oikos* 59 (2), 253. doi: 10.2307/3545542

Kubiszyn, A. M., Piwosz, K., Wiktor, J. M., and Wiktor, J. M. (2014). The effect of inter-annual Atlantic water inflow variability on the planktonic protist community structure in the West spitsbergen waters during the summer. *J. Plankton Res.* 36 (5), 1190–1203. doi: 10.1093/plankt/fbu044

Kubiszyn, A. M., Wiktor, J. M., Wiktor, J. M., Griffiths, C., Kristiansen, S., and Gabrielsen, T. M. (2017). The annual planktonic protist community structure in an ice-free high Arctic fjord (Adventfjorden, West spitsbergen). *J. Mar. Syst.* 169, 61–72. doi: 10.1016/j.jmarsys.2017.01.013

Kuhn, A. M., Dutkiewicz, S., Jahn, O., Clayton, S., Rynearson, T. A., Mazloff, M. R., et al. (2019). Temporal and spatial scales of correlation in marine phytoplankton communities. *J. Geophys. Res. Ocean* 124 (12), 9417–9438. doi: 10.1029/2019JC015331

Levin, S. A., and Segel, L. A. (1976). Hypothesis for origin of planktonic patchiness. *Nature* 259, 659. doi: 10.1038/259659a0.

Lévy, M., Franks, P. J. S., and Smith, K. S. (2018). The role of submesoscale currents in structuring marine ecosystems. *Nat. Commun.* 9 (1), 4758. doi: 10.1038/s41467-018-07059-3

Li, W. K. W., McLaughlin, F. A., Lovejoy, C., and Carmack, E. C. (2009). Smallest algae thrive as the arctic ocean freshens. *Science* 326 (5952), 539. doi: 10.1126/science.1179798

Lombard, F., Boss, E., Waite, A. M., Uitz, J., Stemmann, L., Sosik, H. M., et al. (2019). Appeltans, w.: Globally consistent quantitative observations of planktonic ecosystems. *Front. Mar. Sci.* 6. doi: 10.3389/fmars.2019.00196

Lovejoy, S., Currie, W. J. S., Tessier, Y., Claereboudt, M. R., Bourget, E., Roff, J. C., et al. (2001). Universal multifractals and ocean patchiness: Phytoplankton, physical fields and coastal heterogeneity. *J. Plankton Res.* 23 (2), 117–141. doi: 10.1093/plankt/23.2.117

Lydersen, C., Assmy, P., Falk-Petersen, S., Kohler, J., Kavacs, K. M., Reigstad, M., et al. (2014). The importance of tidewater glaciers for marine mammals and seabirds in Svalbard, Norway. *J. Mar. Syst.* 129, 452–471. doi: 10.1016/j.radphyschem.2014.05.010

Mackas, D. L. (1984). Spatial autocorrelation of plankton community composition in a continental shelf ecosystem. *Limnol. Oceanogr.* 29 (3), 451–471. doi: 10.4319/lo.1984.29.3.0451

Mackas, D. L., Denman, K. L., and Abbott, M. R. (1985). Plankton patchiness: biology in the physical vernacular. *Bull. Mar. Sci.* 37 (2), 653–674.

Mahadevan, A. (2016). The impact of submesoscale physics on primary productivity of plankton. *Ann. Rev. Mar. Sci.* 8 (1), 161–184. doi: 10.1146/annurev-marine-010814-015912

Martin, A. P. (2003). Phytoplankton patchiness: the role of lateral stirring and mixing. *Prog. Oceanogr.* 57 (2), 125–174. doi: 10.1016/s0079-6611(03)00085-5

Matsuoka, A., Bricaud, A., Benner, R., Para, J., Sempéré, R., Prieur, L., et al. (2012). Tracing the transport of colored dissolved organic matter in water masses of the southern Beaufort Sea: relationship with hydrographic characteristics. *Biogeosciences* 9 (3), 925–940. doi: 10.5194/bg-9-925-2012

McGovern, M., Pavlov, A. K., Deininger, A., Granskog, M. A., Leu, E., Søreide, J. E., et al. (2020). Terrestrial inputs drive seasonality in organic matter and nutrient biogeochemistry in a high Arctic fjord system (Isfjorden, Svalbard). *Front. Mar. Sci.* 7. doi: 10.3389/fmars.2020.542563

McManus, M. A., Cheriton, O. M., Drake, P. J., Holliday, D. V., Storlazzi, C. D., Donaghay, P. L., et al. (2005). Effects of physical processes on structure and transport of thin zooplankton layers in the coastal ocean. *Mar. Ecol. Prog. Ser.* 301, 199–215. doi: 10.3354/meps301199

McManus, M., Greer, A., Timmerman, A., Sevadjian, J., Woodson, C., Cowen, R., et al. (2021). Characterization of the biological, physical, and chemical properties of a toxic thin layer in a temperate marine system. *Mar. Ecol. Prog. Ser.* 678, 17–35. doi: 10.3354/meps13879

Meire, L., Mortensen, J., Meire, P., Juul-Pedersen, T., Sejr, M. K., Rysgaard, S., et al. (2017). Marine-terminating glaciers sustain high productivity in Greenland fjords. *Glob. Change Biol.* 23 (12), 5344–5357. doi: 10.1111/gcb.13801

Menden-Deuer, S. (2012). Structure-dependent phytoplankton photosynthesis and production rates: Implications for the formation, maintenance, and decline of plankton patches. *Mar. Ecol. Prog. Ser.* 468, 15–30. doi: 10.3354/meps09968

Metfies, K., Von Appen, W. J., Kilias, E., Nicolaus, A., and Nöthig, E. M. (2016). Biogeography and photosynthetic biomass of arctic marine pico-eukaroytes during summer of the record sea ice minimum 2012. *PLoS One* 11 (2), 1–20. doi: 10.1371/journal.pone.0148512

Möller, K. O., John, M. S., Temming, A., Floeter, J., Sell, A. F., Herrmann, J. P., et al. (2012). Marine snow, zooplankton and thin layers: Indications of a trophic link from small-scale sampling with the video plankton recorder. *Mar. Ecol. Prog. Ser.* 468, 57–69. doi: 10.3354/meps09984

Nayak, A. R., Jiang, H., Byron, M. L., Sullivan, J. M., McFarland, M. N., and Murphy, D. W. (2021). Editorial: Small scale spatial and temporal patterns in particles, plankton, and other organisms. *Front. Mar. Sci.* 8. doi: 10.3389/fmars.2021.669530

Nilsen, F., Cottier, F., Skogseth, R., and Mattsson, S. (2008). Fjord-shelf exchanges controlled by ice and brine production: The interannual variation of Atlantic water in isfjorden, Svalbard. *Cont. Shelf Res.* 28 (14), 1838–1853. doi: 10.1016/j.csr.2008.04.015

Nöthig, E. M., Bracher, A., Engel, A., Metfies, K., Niehoff, B., Peeken, I., et al. (2015). Summertime plankton ecology in fram strait-a compilation of long-and short-term observations. *Polar Res.* 34 (1), 23349. doi: 10.3402/polar.v34.23349

Pavlov, A. K., Tverberg, V., Ivanov, B. V., Nilsen, F., Falk-Petersen, S., and Granskog, M. A. (2013). Warming of Atlantic water in two west spitsbergen fjords over the last century, (1912-2009). *Polar Res.* 32, 1–14. doi: 10.3402/polar.v32i0.11206

Pinel-Alloul, P. (1995). Spatial heterogeneity as a multiscale characteristic of zooplankton community. *Hydrobiologia* 300–301 (1), 17–42. doi: 10.1007/BF00024445

Piontkovski, S. A., Williams, R., Peterson, W. T., Yunev, O. A., Minkina, N. I., Vladimirov, V. L., et al. (1997). Spatial heterogeneity of the planktonic fields in the upper mixed layer of the open ocean. *Mar. Ecol. Prog. Ser.* 148 (1–3), 145–154. doi: 10.3354/meps148145

Piwosz, K., Walkusz, W., Hapter, R., Wieczorek, P., Hop, H., and Wiktor, J. (2009). Comparison of productivity and phytoplankton in a warm (Kongsfjorden) and a cold (Hornsund) spitsbergen fjord in mid-summer 2002. *Polar Biol.* 32 (4), 549–559. doi: 10.1007/s00300-008-0549-2

Prairie, J. C., Franks, P. J. S., and Jaffe, J. S. (2010). Cryptic peaks: Invisible vertical structure in fluorescent particles revealed using a planar laser imaging fluorometer. *Limnol. Oceanogr.* 55 (5), 1943–1958. doi: 10.4319/lo.2010.55.5.1943

Prairie, J. C., Sutherland, K. R., Nickols, K. J., and Kaltenberg, A. M. (2012). Biophysical interactions in the plankton: A cross-scale review. *Limnol. Oceanogr. Fluids Environ.* 2 (1), 121–145. doi: 10.1215/21573689-1964713

Priyadarshi, A., Smith, S. L., Mandal, S., Tanaka, M., and Yamazaki, H. (2019). Micro-scale patchiness enhances trophic transfer efficiency and potential plankton biodiversity. *Sci. Rep.* 9 (1), 1–9. doi: 10.1038/s41598-019-53592-6

Reynolds, R. A., Stramski, D., Wright, V. M., and Woźniak, S. B. (2010). Measurements and characterization of particle size distributions in coastal waters. *J. Geophys. Res. Ocean* 115 (8), C08024. doi: 10.1029/2009JC005930

Robinson, K. L., Sponaugle, S., Luo, J. Y., Gleiber, M. R., and Cowen, R. K. (2021). Big or small , patchy all : Resolution of marine plankton patch structure at micro- to submesoscales for 36 taxa. *Sci. Adv.* 7, 2904. doi: 10.1126/sciadv.abk2904

Schlitzer, R. (2018). *Ocean Data View*. Available at: https://odv.awi.de

Schmitt, F. G., and Seuront, L. (2008). Intermittent turbulence and copepod dynamics: Increase in encounter rates through preferential concentration. *J. Mar. Syst.* 70 (3–4), 263–272. doi: 10.1016/j.jmarsys.2007.01.008

Seuront, L., Schmitt, F., and Lagadeuc, Y. (2001). Turbulence intermittency, small-scale phytoplankton patchiness and encounter rates in plankton: Where do we go from here? *Deep Res. Part I Oceanogr. Res. Pap* 48 (5), 1199–1215. doi: 10.1016/S0967-0637(00)00089-3

Skogseth, R., Olivier, L. L. A., Nilsen, F., Falck, E., Fraser, N., Tverberg, V., et al. (2020). Variability and decadal trends in the isfjorden (Svalbard) ocean climate and circulation – an indicator for climate change in the European Arctic. *Prog. Oceanogr.* 187, 102394. doi: 10.1016/j.pocean.2020.102394

Smith, R. W., Bianchi, T. S., Allison, M., Savage, C., and Galy, V. (2015). High rates of organic carbon burial in fjord sediments globally. *Nat. Geosci.* 8 (6), 450–453. doi: 10.1038/NGEO2421

Smoła, Z. T., Tatarek, A., Wiktor, J. M. W., Wiktor, J. M. W., Kubiszyn, A., and Węsławski, J. M. (2017). Primary producers and production in hornsund and kongsfjorden - comparison of two fjord systems. *Polish Polar Res.* 38 (3), 351–373. doi: 10.1515/popore-2017-0013

Stacey, M. T., McManus, M. A., and Steinbuck, J. V. (2007). Convergences and divergences and thin layer formation and maintenance. *Limnol. Oceanogr.* 52 (4), 1523–1532. doi: 10.4319/lo.2007.52.4.1523

Stanley, R. H. R., McGillicuddy, D. J., Sandwith, Z. O., and Pleskow, H. M. (2017). Submesoscale hotspots of productivity and respiration: Insights from high-resolution oxygen and fluorescence sections. *Deep Res. Part I Oceanogr. Res. Pap* 130, 1–11. doi: 10.1016/j.dsr.2017.10.005

Steinbuck, J. V., Stacey, M. T., McManus, M. A., Cheriton, O. M., and Ryan, J. P. (2009). Observations of turbulent mixing in a phytoplankton thin layer: Implications for formation, maintenance, and breakdown. *Limnol. Oceanogr.* 54 (4), 1353–1368. doi: 10.4319/lo.2009.54.4.1353

Stemmann, L., and Boss, E. (2012). Plankton and particle size and packaging: From determining optical properties to driving the biological pump. *Ann. Rev. Mar. Sci.* 4 (1), 263–290. doi: 10.1146/annurev-marine-120710-100853

Stemmann, L., Eloire, D., Sciandra, A., Jackson, G. A., Guidi, L., Picheral, M., et al. (2008). Volume distribution for particles between 3.5 to 2000µm in the upper 200m region of the south pacific gyre. *Biogeosciences* 5 (2), 299–310. doi: 10.5194/bg-5-299-2008

Svendsen, H., Beszczynska-Møller, A., Hagen, J. O., Lefauconnier, B., Tverberg, V., Gerland, S., et al. (2002). The physical environment of kongsfjorden – krossfjorden, an Arctic fjord system in Svalbard. *Polar Res.* 21 (1), 133–166. doi: 10.1111/j.1751-8369.2002.tb00072.x

Svensen, C., Halvorsen, E., Vernet, M., Franzè, G., Dmoch, K., Lavrentyev, P. J., et al. (2019). Zooplankton communities associated with new and regenerated

primary production in the Atlantic inflow north of Svalbard. *Front. Mar. Sci.* 6. doi: 10.3389/fmars.2019.00293

Szeligowska, M., Trudnowska, E., Boehnke, R., Dąbrowska, A. M., Dragańska-Deja, K., Deja, K., et al. (2021). The interplay between plankton and particles in the isfjorden waters influenced by marine- and land-terminating glaciers. *Sci. Total Environ.* 780, 146491. doi: 10.1016/j.scitotenv.2021.146491

Szeligowska, M., Trudnowska, E., Boehnke, R., Dąbrowska, A. M., Wiktor, J. M., Sagan, S., et al. (2020). Spatial patterns of particles and plankton in the warming Arctic fjord (Isfjorden, West spitsbergen) in seven consecutive mid-summers, (2013–2019). *Front. Mar. Sci.* 7 (584). doi: 10.3389/fmars.2020.00584

Timmerman, A. H. V., McManus, M. A., Cheriton, O. M., Cowen, R. K., Greer, A. T., Kudela, R. M., et al. (2014). Hidden thin layers of toxic diatoms in a coastal bay. *Deep Res. Part II Top. Stud. Oceanogr.* 101, 129–140. doi: 10.1016/j.dsr2.2013.05.030

Trudnowska, E., Basedow, S. L., and Blachowiak-Samolyk, K. (2014). Mid-summer mesozooplankton biomass, its size distribution, and estimated production within a glacial Arctic fjord (Hornsund, Svalbard). *J. Mar. Syst.* 137, 55–66. doi: 10.1016/j.jmarsys.2014.04.010

Trudnowska, E., Dąbrowska, A. M., Boehnke, R., Zajączkowski, M., and Blachowiak-Samolyk, K. (2020a). Particles, protists, and zooplankton in glacier-influenced coastal svalbard waters. *Estuar. Coast. Shelf Sci.* 242, 106842. doi: 10.1016/j.ecss.2020.106842

Trudnowska, E., Gluchowska, M., Beszczynska-Möller, A., Blachowiak-Samolyk, K., and Kwasniewski, S. (2016). Plankton patchiness in the polar front region of the west spitsbergen shelf. *Mar. Ecol. Prog. Ser.* 560, 1–18. doi: 10.3354/meps11925

Trudnowska, E., Sagan, S., and Błachowiak-Samołyk, K. (2018). Spatial variability and size structure of particles and plankton in the fram strait. *Prog. Oceanogr.* 168, 1–12. doi: 10.1016/j.pocean.2018.09.005

Trudnowska, E., Stemmann, L., Błachowiak-Samołyk, K., and Kwasniewski, S. (2020b). Taxonomic and size structures of zooplankton communities in the fjords along the Atlantic water passage to the Arctic. *J. Mar. Syst.* 204. doi: 10.1016/j.jmarsys.2020.103306

Trudnowska, E., Szczucka, J., Hoppe, L., Boehnke, R., Hop, H., and Blachowiak-Samolyk, K. (2012). Multidimensional zooplankton observations on the northern West spitsbergen shelf. *J. Mar. Syst.* 98–99, 18–25. doi: 10.1016/j.jmarsys.2012.03.001

Urbanski, J. A., Stempniewicz, L., Weslawski, J. M., Draganska-Deja, K., Wochna, A., Goc, M., et al. (2017). Subglacial discharges create fluctuating foraging hotspots for sea birds in tidewater glacier bays. *Sci. Rep.* 7, 43999. doi: 10.1038/srep43999

Vihtakari, M., Welcker, J., Moe, B., Chastel, O., Tartu, S., Hop, H., et al. (2018). Black-legged kittiwakes as messengers of atlantification in the Arctic. *Sci. Rep.* 8 (1), 1–11. doi: 10.1038/s41598-017-19118-8

Vihtakari, M.. (2019). PlotSvalbard: PlotSvalbard – Plot research data from Svalbard on maps. *R Package Version 0.8.5*. Available at: https://github.com/MikkoVihtakari/PlotSvalbard

Villarino, E., Watson, J. R., Jönsson, B., Gasol, J. M., Salazar, G., Acinas, S. G., et al. (2018). Large-Scale ocean connectivity and planktonic body size. *Nat. Commun.* 9 (1), 142. doi: 10.1038/s41467-017-02535-8

Węsławski, J. M., Buchholz, F., Głuchowska, M., and Weydmann, A. (2017). Ecosystem maturation follows the warming of the Arctic fjords. *Oceanologia* 59 (4), 592–602. doi: 10.1016/j.oceano.2017.02.002

White, A. E., Letelier, R. M., Whitmire, A. L., Barone, B., Bidigare, R. R., Church, M. J., et al. (2015). Phenology of particle size distributions and primary productivity in the north pacific subtropical gyre (Station ALOHA) angelicque. *J. Geophys. Res. Ocean* 120, 7381–7399. doi: 10.1002/2015JC010897.Received

Wiebe, P. H. (1970). Small-scale spatial distribution oceanic zooplankton. *Limnol. Oceanogr.* 15 (2), 205–217. doi: 10.4319/lo.1970.15.2.0205

Wiebe, P. H., Wiebe, P. H., and Holland, W. R. (1968). Plankton patchiness: Effects on repeated net tows. *Limnol. Oceanogr.* 13 (2), 315–321. doi: 10.4319/lo.1968.13.2.0315

Wiencke, C., and Hop, H. (2016). Ecosystem kongsfjorden: new views after more than a decade of research. *Polar Biol.* 39 (10), 1679–1687. doi: 10.1007/s00300-016-2032-9

Zaborska, A., Włodarska-Kowalczuk, M., Legeżyńska, J., Jankowska, E., Winogradow, A., and Deja, K. (2018). Sedimentary organic matter sources, benthic consumption and burial in west spitsbergen fjords – signs of maturing of Arctic fjordic systems? *J. Mar. Syst.* 180, 112–123. doi: 10.1016/j.jmarsys.2016.11.005

Zhou, M. (2006). What determines the slope of a plankton biomass spectrum? *J. Plankton Res.* 28 (5), 437–448. doi: 10.1093/plankt/fbi119

Zhou, M., Carlotti, F., and Zhu, Y. (2010). A size-spectrum zooplankton closure model for ecosystem modelling. *J. Plankton Res.* 32 (8), 1147–1165. doi: 10.1093/plankt/fbq054